Mobile trap algorithm for zinc detection using protein sensors

Munish V. Inamdar
Department of Mechanical Engineering, University of Michigan, Ann Arbor, Michigan 48109-2125, USA

Christian M. Lastoskie
Department of Civil and Environmental Engineering, University of Michigan, Ann Arbor, Michigan 48109-2125, USA and Department of Biomedical Engineering, University of Michigan, Ann Arbor, Michigan 48109-2099, USA

Carol A. Fierke
Department of Chemistry, University of Michigan, Ann Arbor, Michigan 48109-1055, USA

Ann Marie Sastry[a)]
Department of Mechanical Engineering, University of Michigan, Ann Arbor, Michigan 48109-2125, USA; Department of Biomedical Engineering, University of Michigan, Ann Arbor, Michigan 48109-2099, USA; and Department of Materials Science and Engineering, University of Michigan, Ann Arbor, Michigan 48109-2136, USA

(Received 14 May 2007; accepted 9 August 2007; published online 8 November 2007)

We present a mobile trap algorithm to sense zinc ions using protein-based sensors such as carbonic anhydrase (CA). Zinc is an essential biometal required for mammalian cellular functions although its intracellular concentration is reported to be very low. Protein-based sensors like CA molecules are employed to sense rare species like zinc ions. In this study, the zinc ions are mobile targets, which are sought by the mobile traps in the form of sensors. Particle motions are modeled using random walk along with the first passage technique for efficient simulations. The association reaction between sensors and ions is incorporated using a probability (p_1) upon an ion-sensor collision. The dissociation reaction of an ion-bound CA molecule is modeled using a second, independent probability (p_2). The results of the algorithm are verified against the traditional simulation techniques (e.g., Gillespie's algorithm). This study demonstrates that individual sensor molecules can be characterized using the probability pair (p_1,p_2), which, in turn, is linked to the system level chemical kinetic constants, k_{on} and k_{off}. Further investigations of CA-Zn reaction using the mobile trap algorithm show that when the diffusivity of zinc ions approaches that of sensor molecules, the reaction data obtained using the static trap assumption differ from the reaction data obtained using the mobile trap formulation. This study also reveals similar behavior when the sensor molecule has higher dissociation constant. In both the cases, the reaction data obtained using the static trap formulation reach equilibrium at a higher number of complex molecules (ion-bound sensor molecules) compared to the reaction data from the mobile trap formulation. With practical limitations on the number sensors that can be inserted/expressed in a cell and stochastic nature of the intracellular ionic concentrations, fluorescence from the number of complex sensor molecules at equilibrium will be the measure of the intracellular ion concentration. For reliable detection of zinc ions, it is desirable that the sensors must not bind all the zinc ions tightly, but should rather bind and unbind. Thus for a given fluorescence and with association-dissociation reactions between ions and sensors, the static trap approach will underestimate the number of zinc ions present in the system. © *2007 American Institute of Physics*. [DOI: 10.1063/1.2778684]

I. INTRODUCTION

While zinc is the second most abundant intracellular trace metal ion, with well-established and essential physiological roles, vanishingly small concentrations of rapidly exchangeable intracellular zinc have been found in mammalian[1] and bacterial[2,3] cells (summarized by Table I, following Refs. 4–9). Zinc is critical to both catalytic and structural functions of proteins,[10] and plays an important role in protein folding,[11–13] but its reactivity and toxicity during uncontrolled release are well documented. Zinc fluxes have been linked to Alzheimer's disease[14] and to other forms of neurological damage.[15,16] The low concentration of readily exchangeable zinc in cells may thus be explained by the need for its tight control. But from a modeling standpoint, such tight regulation may prohibit the application of standard characterization of fluxes in a diffusion framework, as used for other intracellular ions, e.g., calcium.[17–19]

Measurement of intracellular zinc has been principally accomplished using protein-based sensors wherein affinity of the sensors is expressed as the equilibrium dissociation constant K_D,[20] the ratio of two kinetic constants k_{off}/k_{on}. Proteins

[a)]Author to whom correspondence should be addressed. Electronic mail: amsastry@umich.edu

TABLE I. Prior work in measurement of intracellular zinc concentration.

Authors	Year	Cell type	Method	Intracellular zinc concentration
Simons (Ref. 4)	1991	Human red blood cell	Radioactive ^{65}Zn	24 pM
Atar *et al.* (Ref. 5)	1995	Heart cells	Fura-2 and UV fluorescence	1 nM
Benters *et al.* (Ref. 6)	1997	E367 neuroblastoma cells	5F-BAPTA and ^{19}F-NMR spectra	0.5 nM
Sensi *et al.* (Ref. 7)	1997	Cortical neurons	Magfura-5 and UV fluorescence	2 nM
Haase and Beyensmann (Ref. 8)	1999	C6 rat glioma cells	Zinquin and UV fluorescence	Increases in extracellular zinc concentration beyond 200 mM, did not change intracellular zinc ion concentration
Bozym *et al.* (Ref. 9)	2006	PC-12 (rat pheochromocytoma)	Carbonic anhydrase and fluorescence	5–10 pM

used in this way are referred to as sensors, binders, or sensing proteins. The constant $k_{on}(M^{-1}\ s^{-1})$, the association rate or the *on rate constant*, is a measure of the speed with which a sensing protein binds a biometal ion, and $k_{off}(s^{-1})$, the dissociation rate constant, is a measure of the time dependent tendency of a complex (protein-ion) molecule to dissociate back into its reactant particles. The fundamentals of this approach can be described briefly as follows, using carbonic anhydrase (CA). This protein has been used to sense zinc[20,21] because of its high sensitivity and selectivity for zinc ions, tunable affinity for zinc, and the ability to couple zinc binding to the binding of a fluorescent sulfonamide ligand; specific properties are summarized in Table II.[22–29] A typical reaction between CA molecules and zinc ions can be written simply as

$$\mathrm{CA} + \mathrm{Zn} \underset{k_{off}}{\overset{k_{on}}{\leftrightarrow}} \mathrm{CA-Zn}. \tag{1}$$

In prior experiments, K_D was estimated by dialyzing apo-CA (i.e., CA without bound zinc) with excess zinc ions in a suitable *p*H and metal ion buffer solution (see Ref. 23, for example). After sufficient incubation to assure equilibrium, the amounts of total CA and enzyme-bound Zn (E-Zn) were quantified after addition of the sulfonamide fluorophore and measuring its fluorescence. This procedure was repeated for various values of free zinc concentrations. The dependence of the concentration of E-Zn as a function of free zinc concentration was then fitted to Eq. (2) using a fitting constant C, whereupon K_D was obtained, as

$$\frac{[E\text{-Zn}]}{[E]_{tot}} = \frac{C}{1 + K_D/[\mathrm{Zn}]_{free}}. \tag{2}$$

To estimate k_{off} time dependent dissociation of zinc ions from a solution of holo-CA (i.e., CA with bound zinc) was observed (see Ref. 23, for example). At regular time intervals, the E-Zn was quantified and k_{off} was obtained via

$$\frac{[E\text{-Zn}]}{[E]_{tot}} = A_0 e^{-k_{off}t}. \tag{3}$$

The remaining kinetic constant, k_{on}, was then calculated as the ratio k_{off}/K_D, assuming a simple *ligand binding reaction*.

Modeling zinc exchange through direct simulation is highly desirable given its critical role in normal physiologic and disease states. We prefer the terminology "readily exchangeable" rather than "free" zinc, simply because the measured zinc concentration in any experiment is irrevocably tied to the affinity of the sensing species to the ion, relative to other possible binders. And though a diffusive framework has been used in characterizing experimental zinc binding, single binding events themselves are the result of possibly complex combination of path of approach, nearness, and the state of protein/ion combination preceding a collision,[30–32] as with other reactions. Further, unbinding of an ion also depends on the above physical factors.[30]

Earlier work in the reaction modeling includes theoretical studies of reactions using diffusion equation, Monte Carlo simulations, and Brownian dynamics simulations. The reactant particles in these studies are often treated as targets and traps. Northrup *et al.*[33,34] used Brownian dynamics to simulate a reaction between an enzyme particle and a substrate. Monte Carlo simulations have been used[35,36] to simulate reactions between particles and also have been used to estimate the survival time of a target (the time of free existence before the target is captured by a trap) surrounded by a number of static traps.[37–41] Probability theory has been used to conduct theoretical analyses of the survival time of

TABLE II. Experimentally determined K_D and k_{off} values for various variants of human carbonic anhydrase. Asterisks indicate unreported values.

Authors	Year	CAII variant	K_D (pM)	k_{off} (h^{-1})
Kiefer and Fierke (Ref. 22)	1994	His94Ala	270 000	⩾140
		His94Cys	33 000	0.5
Keifer *et al.* (Ref. 23)	1995	Q92A	18	1.6
		Q92L	30	0.12
		Q92N	5	2.6
Ippolito *et al.* (Ref. 24)	1995	T199D	4	*
		T199H	77	*
Huang *et al.* (Ref. 25)	1996	E117Q	4 000	4680
Lesburg *et al.* (Ref. 26)	1997	H119N	11 000	9
		H119Q	70 000	6
Hunt and Fierke (Ref. 27)	1997	FHMHV	1.6	2.1
		MHLHW	10	0.8
Thompson *et al.* (Ref. 28)	2002	L198C	58	*
McCall and Fierke (Ref. 29)	2004	H94D	8	*
		H94N	5	*

targets.[42–46] Two equivalent algorithms[47,48] have been used to simulate a kinetic reaction using the kinetic constants k_{on} and k_{off}, with the central aim of simulating stochastic "noise" in certain biological phenomena. The diffusion equation has been solved around a stationary particle to obtain the expressions for k_{on};[49,50] a recent review[51] has appeared on these techniques.

Here, we aim to directly simulate binding events, specifically for zinc-CA binding, using a novel approach to overcome some of the difficulties in prior work at the atomistic scale,[30,33,34,52] using probabilistic modeling. We further aim to provide several missing elements specific to the zinc-CA problem.

Probabilistic techniques must account for large differences in the speed of the reactants in a medium. CA, with a molecular weight (M) of 40 kD and the radius of gyration (R_G) of 16.13 Å (please refer to Sec. II for the details of a CA molecule dimension), at 300 K (T), can be estimated to diffuse in water at a rate of 9.18×10^{-11} m^2/s,[53] obtained using Eq. (4),

$$D = 6.85 \times 10^{-15} T/\eta\sqrt{M^{1/3}R_G}. \tag{4}$$

While zinc ions can be estimated to diffuse at a rate of 2.19×10^{-9} m^2/s under the above mentioned conditions, using Eq. (5),

$$D = \frac{k_b T}{6\pi\eta R_H}. \tag{5}$$

Prior, direct stochastic simulations of particle interactions[35,54] carried out on a two dimensional (2D), equispaced grid cannot be readily extended to species of widely varying mobility. Further, continuum approaches (i.e., simulations in which reactant particles execute random walks in a homogeneous medium) of direct stochastic simulations of the particle interactions with different diffusion coefficients[36] employ a constant step for all particle motions; for the heterogeneous zinc-CA system, this methodology could lead to missing some particle collisions.

Probabilistic techniques should properly simulate both the association and dissociation of CA molecules and zinc ions, all of which are mobile in a three dimensional (3D) space. With the nature of the cellular cytosol being debated, the principal texts on cellular biology (e.g., Ref. 13) still suggest ionic transport in three dimensional (3D). Specific pathways and trajectories for zinc (and other highly reactive ions) are not yet conclusively established but their existence had been proposed.[52] In the presence of such diverse opinions, we decided to develop our algorithm for the general case of 3D transport of zinc ions.

For the zinc-CA system modeled at the particle level, we expect that the probability of association and dissociation should remain constant, as long as there are no external agents that force CA molecules to abruptly change their conformations. In prior stochastic approaches (e.g., Gillespie's algorithm[47,55,56] and STOCHSIM[48]), global probabilities of reactions do not remain constant in time, nor do these algorithms consider spatial positions and motions of the reacting particles. Existing Monte Carlo techniques that simulate a reaction between two types of particles either with immediate reaction upon collision[38,39,56] or with a probability of association upon collision[40] are restricted to the reaction between the mobile species (targets) and the stationary species (traps). Theoretical probabilistic techniques, studying reactions between two types of particles, have so far been limited to grid,[42] one-dimensional systems,[43,44] systems involving a single and stationary target reacting with a group of mobile traps, or vice versa.[41,45,46,57] Other techniques involve derivation of survival probability of reacting particles and indirectly implement the probabilities of association and dissociation.[58] But a probabilistic technique that accounts for association and dissociation probabilities independently is required for a number of reacting particles in a 3D continuum system.

Techniques involving long simulation times, suitable for comparison with experiments, are critically needed in verifying kinetic assumptions. Techniques involving detailed random walks of species[59,60] are computationally intensive because they use a very small time increment for particle position updating. These techniques, such as Brownian dynamics simulations,[33,34,61] simulate a reaction between an enzyme and a substrate. As with other approaches, these techniques to date have not considered probabilistic dissociation.

Direct insertion of reaction probabilities obtained through atomistic simulation is highly desirable, given the rapidly expanding capabilities of modeling individual binding events. Gillespie's algorithm[47] and STOCHSIM[48] do not employ reaction probabilities at the particle level. Rather these algorithms employ the kinetic constants k_{on} and k_{off}, and the number of reactant particles, to estimate these probabilities. In Monte Carlo techniques and theoretical probabilistic studies, only the probability of association was incorporated, and only in the special cases that we mentioned earlier.

The ability to sense zinc in both water and in the cytosol is essential. In water, a zinc ion is approximately 24 times more mobile than a CA molecule. But in the cytosol, the zinc ion is actively chelated.[62] Depending on the medium, the CA molecules and the zinc ions may have substantially different relative speeds. Employing the static trap technique alone to model the zinc-protein (CA) reaction by immobilization of the CA molecules is an oversimplification of the system.

Our present approach addresses this problem using a stochastic framework proposed earlier.[62,63] Our objectives in the present work were as follows:

(1) To implement and verify a stochastic computational algorithm using probabilities of association and dissociation to determine the fate of reactant particles, assuming all reactant particles to be mobile in 3D, with individual speeds (depending on particle mass and temperature of the system).
(2) To use the algorithm to simulate the zinc-CA reaction in solution with excess protein molecules, using physically plausible speeds of protein molecules and ions, to determine the probabilities of association (using the experimental value of k_{on}) and disassociation (using the

probability of association and the experimental value of k_{off}).

(3) To study the effect of relative speed of zinc ions on the zinc-CA reaction when CA molecules are mobile and stationary, thereby determining the limits of application of static trap algorithms for this reaction.

II. METHODS

A. Assumptions and implementation of the mobile trap algorithm

Our simulation procedure is described in the context of the zinc-CA system. Zinc ions are modeled as mobile targets, and CA molecules as mobile traps. We refer to our implementation as a "mobile trap" algorithm to differentiate it from previous mobile target-static trap approaches (e.g., Ref. 38). Green's function formulation has been developed[64] for the chemical kinetics but the methodology of the random walk allows us to implement the first passage principle which in turn allows us to write the exact expression for the average time required for a diffusive particle to travel a distance. This distance of travel can be linked to the positions of the reacting particles and hence collisions can be detected more accurately as described in the subsequent paragraphs.

A set of key assumptions follows here. Reactions are assumed to take place in stationary water, the reactant zinc ions and CA molecules are assumed to be "well mixed," and the motions of particles are considered to be uncorrelated. Particle motions are assumed to result solely from thermal energy and are thus modeled as random walks. The mass of system remains constant, and thus, the time dependent variation of the complex molecules obeys the law of mass action. CA molecules and zinc ions are initially distributed randomly in the simulation domain. Interactions among zinc ions are neglected.

We use random walks to simulate particle motions. Simulating individual step random walks is very time consuming, and hence the first passage methodology is used to speed up the simulations. Particles that execute a random walk must obey the first passage rule[37]

$$P(\tau,x=0;R)=1+2\sum_{n=0}^{\infty}(-1)^n \exp(-Dn^2\pi^2\tau/R^2), \qquad (6)$$

where $P(\tau,x=0;R)$ is the probability that a particle starting at the center of sphere $(x=0)$ reaches the surface of the prescribed sphere of radius R for the first time after time τ. The expected value of τ can be obtained by integrating Eq. (6), i.e.,

$$\bar{\tau}=\int_0^{\infty}\frac{dP}{d\tau}d\tau=\frac{R^2}{6D}. \qquad (7)$$

Equation (7) holds for individual particles, zinc ions as well as CA molecules. When CA and zinc particles react, the distance R will be the neighbor distance that permits the event of a collision between the reacting particles in a time $\bar{\tau}$.

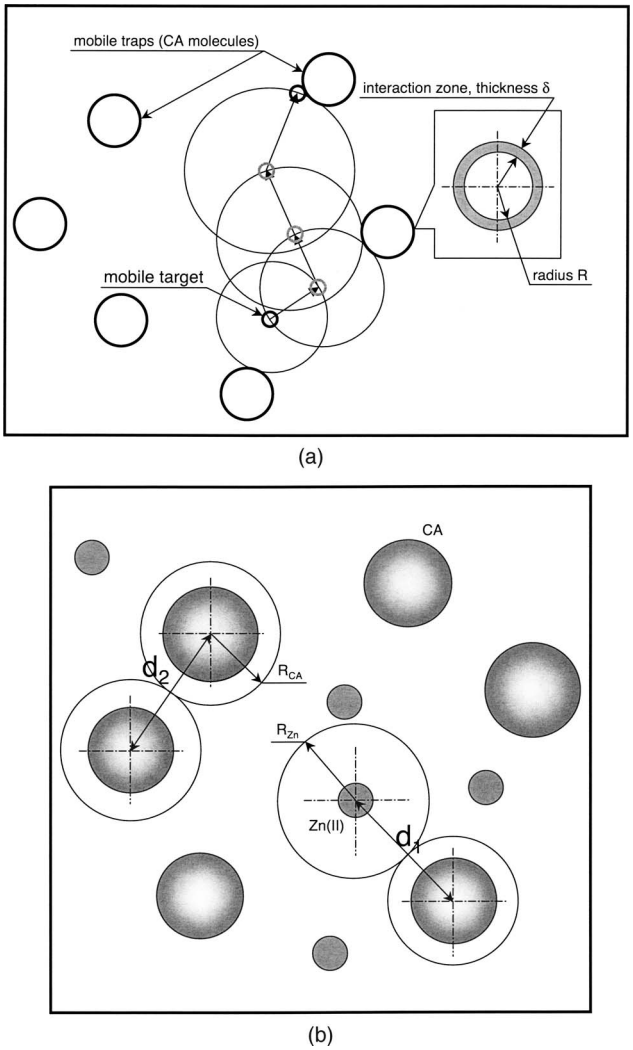

FIG. 1. (a) Movement of a zinc ion (smaller circle) through randomly distributed CA molecules (larger circles) and binding to a CA molecule. The paths of CA molecules are not shown. (b) Various variables used in simulations that are obtained from the current particle positions.

Collisions are detected using zones of influence around mobile traps. We note that we use the term "collide" to refer to collocation of particles within a zone of interaction of one another. This zone comprises a radial thickness δ, around a CA molecule, expressed as

$$\delta=fR_{CA} \quad 0<f<1, \qquad (8)$$

where R_{CA} is the radius of a CA molecule.

The first passage approach and the collision detection condition are used to simulate the interplay between zinc ions and CA molecules. A CA molecule is modeled as a sphere of 25.5 Å radius (corresponding to E117Q structure[65]) and a zinc ion is modeled as a particle of negligible size.

Our algorithm dynamically selects time steps such that only one collision would take place either between a free zinc ion and a free CA molecule or between two apo- or holo-CA molecules (Fig. 1). First, two types of minimum distances are obtained from the instantaneous particle positions:

(1) d_1, the minimum distance between two CA molecules (apo or holo) and
(2) d_2, the minimum distance between a free CA molecule and a zinc ion.

Then the expected times, required to travel d_1 and d_2 by the participating particles, so that they can collide, are given by

$$d_1^2 = 24 D_{\mathrm{CA}} t_1, \tag{9}$$

$$d_2^2 = 6 t_2 (D_{\mathrm{Zn}} + D_{\mathrm{CA}} + 2\sqrt{D_{\mathrm{Zn}} D_{\mathrm{CA}}}), \tag{10}$$

where D_{Zn} and D_{CA} are the diffusion coefficients of a zinc ion and a CA molecule, respectively. Equations (9) and (10) are direct outcomes of Eq. (7) applied to mobile particles. The minimum between t_1 and t_2 (denoted by t henceforth) ensures that during the time interval t, only one collision is possible either between CA molecules or between a free zinc ion and a CA molecule, depending on which one of t_1 and t_2 is less.

After the t estimation from the current positions of particles, all CA molecules are moved to a random point on the surface of the spheres whose radii are given by

$$r_{\mathrm{CA}} = \sqrt{6 D_{\mathrm{CA}} t} \tag{11}$$

and all zinc ions are moved to a random point on the surface of the spheres whose radii are given by

$$r_{\mathrm{Zn}} = \sqrt{6 D_{\mathrm{Zn}} t}. \tag{12}$$

Each particle has its own such sphere centered at the current location of center of the particle. The distances between all pairs of a free zinc ion and a free CA molecule are calculated for the collision check. The procedure is repeated and the simulation is carried out for the specified time duration.

In modeling the zinc-CA reaction to incorporate stochastic interactions, the conventional chemical equation [Eq. (1)] is rewritten as

$$\mathrm{CA} + \mathrm{Zn} \underset{p_2}{\overset{p_1}{\leftrightarrow}} \mathrm{CA} - \mathrm{Zn}. \tag{13}$$

The probability of association, p_1, determines binding based on the availability of a binding site and correct mutual orientation of the zinc and CA trajectories at collision. The probability of dissociation, p_2, determines dissociation of complex molecules to its reactant particles. The probability of dissociation is the same for every instant of time.[66] The probabilities (p_1, p_2) are defined at the particle interaction level unlike k_{on} and k_{off} which are system level constants.

The zinc-CA association events are implemented in the mobile trap algorithm with the help of p_1. Whenever a free zinc ion collides with a free CA molecule, a random number is generated to simulate p_1. If the generated random number is less than p_1, then the CA molecule is assigned *occupied* status and the collided zinc ion is moved along with the CA molecule until the occupied CA molecule dissociates. The dissociation of a complex molecule is implemented as follows.

Before the estimation of the distances d_1 and d_2, a CA molecule is selected randomly. If the selected CA molecule is occupied, then a random number is generated to simulate p_2. If the generated random number is less than p_2, then the selected CA molecule is assigned *free* status and the algorithm continues with calculating d_1, d_2, t_1, t_2, and the rest of the stages. The dissociation event is checked before the association event so as to prevent the dissociation of a complex molecule that would be formed without getting the association event unrecorded. A CA molecule is selected for dissociation after every t time interval and the simulation of association-dissociation events is carried out until the prescribed time is reached. During a simulation, the values of each time increment (i.e., t's) and the number of increments are stored. When the simulation ends, the average time increment is obtained by dividing the sum of individual time increments by the total number of increments and this average value of t is referred to as t_{dis} henceforth. The t_{dis} and p_2 values are then used to estimate the value of k_{off}.

B. Verification of implementation: Satisfaction of the law of mass action

The rates of chemical reactions obey the law of mass action (mass balance law),[30,67] which states that the rate of reaction is directly proportional to the product of the concentrations of the reactants. For a general reaction involving two reactants A and B, and the product C, the law of mass action is written as

$$\frac{d[C]}{dt} = k[A][B], \tag{14}$$

where k is the on rate constant. When N_{A0} number of A particles react with N_{B0} number of B particles, the solution to Eq. (14) is

$$N_C = N_{A0} \frac{1 - e^{Kt(N_{A0} - N_{B0})}}{1 - (N_{A0}/N_{B0}) e^{Kt(N_{A0} - N_{B0})}}, \tag{15}$$

where N_C is the number of C particles present at time t, V is the system volume, and A is Avogadro's number. K is given by

$$K = \frac{k}{VA}. \tag{16}$$

The uncertainty analysis[68] of k can also be carried out using the following equation:

$$\Delta N_C = \frac{\partial N_C}{\partial k} w_k = \frac{\partial N_C}{\partial K} \frac{\partial K}{\partial k} w_k = \frac{w_k}{VA} \frac{\partial N_C}{\partial K}, \tag{17}$$

where ΔN_C is the uncertainty in N_C due to the uncertainty w_k in k. Uncertainties in the values of other parameters are neglected. The mobile trap algorithm gives the reaction data (i.e., number of product molecules as a function of time) and these data for various values of N_{A0} and N_{B0} are verified using Eqs. (15) and (17).

C. Correlations between p_1 and k_{on} and between p_2 and k_{off}

The law of mass action for CA-zinc forward reaction is

$$\frac{d[\mathrm{CA}-\mathrm{Zn}]}{dt} = k_{on}[\mathrm{CA}][\mathrm{Zn}]. \tag{18}$$

The left hand side of Eq. (18) is the slope of reaction data curve. When the first zinc-CA complex is formed, the straight line, joining the reference system origin and the point on the reaction data plot corresponding to the first complex molecule formation, represents the initial rate of reaction. As a limiting case, if we study the interaction of a zinc ion with a number of CA molecules, then Eq. (18) reduces to

$$\frac{1}{dt} = k_{on}[\mathrm{CA}]. \tag{19}$$

Equation (19) shows that the rate with which first zinc-CA complex molecule would form is simply the reciprocal of the survival time (dt) of the zinc ion in the mobile pool of CA molecules. From the theory of chemical kinetics, k_{on} is a constant as long as the temperature and the pressure of the system remain constant. Hence we obtain the survival time of a zinc ion for various values of CA concentrations using the mobile trap algorithm and then, $(1/dt)$ versus [CA] data is curve fitted using a straight line to obtain k_{on} (the slope of the line). Alternatively a rectangular hyperbola can be fitted into dt versus [CA] data and the constant of the curve would be a measure of k_{on}.

To obtain the relationship between p_2 and k_{off}, we develop separate selective dissociation simulations and we use the t_{dis} value that is obtained from the mobile trap simulations. A group of zinc-CA complex molecules is considered for the dissociation reaction and the number of zinc-CA complex molecules is the same as the number of CA molecules used in the corresponding mobile trap simulations. A complex molecule is chosen at random from the initial pool. If the chosen molecule is a complex one, then a random number is generated (ran2) to simulate p_2. If ran2 is less than p_2, then the selected molecule is assigned free status. The dissociated zinc ion is assumed to be chelated by other agents; therefore the free CA molecule does not become a complex one during the rest of the simulation. If the selected molecule is not a complex one then no dissociation takes place during that step. The number of free CA molecules and corresponding step numbers are recorded. We repeat the selection-probabilistic dissociation-recording steps until all complex molecules are free. The time duration between two successive selections is t_{dis}. If it takes n steps to dissociate a group of complex molecules then the total physical time required for the reaction is n times t_{dis}. The number of free CA molecules versus time data is curve fitted using Eq. (20) and the k_{off} value is extracted:

$$N_{\mathrm{CA}}(t) = N_{\mathrm{CA0}}(1 - e^{-k_{off}t}), \tag{20}$$

where $N_{\mathrm{CA}}(t)$ is the number free CA molecules at time t and N_{CA0} is the number of complex CA molecules present at time $t=0$. The uncertainty analysis for the k_{off} value is also carried out as per Eq. (21) and

$$\Delta N_{\mathrm{CA}}(t) = \frac{\partial N_{\mathrm{CA}}(t)}{\partial k_{off}} w_{k_{off}}. \tag{21}$$

In order to verify that the probability pair (p_1, p_2) yields same results as those obtained using the kinetic constant pair (k_{on}, k_{off}), the reaction data generated by the mobile trap algorithm using (p_1, p_2) pair are compared with the reaction data generated by Gillespie's algorithm using the corresponding (k_{on}, k_{off}) pair. We note that during mobile trap and selective dissociation simulations, a CA molecule is chosen at random for possible dissociation. We can also check all CA molecules for possible solutions. But random selection of one CA molecule saves the computational time. Also, for a CA molecule with finite dissociation constant, both the methods of CA molecule selection are equivalent. Please see Appendix for the details.

The reaction probability pair (p_1, p_2) can be correlated to either phenomenological rate constants or the intrinsic rate constants.[69] But these rate constants are correlated to each other[64] and the phenomenological kinetic constants are experimentally determined. The accuracy of the intrinsic kinetic constants depends on the accurate estimation of the reaction distance, which is not known in the case of CA. Hence in order to demonstrate the mobile trap algorithm, we have chosen the phenomenological rate constants to correlate the reaction probability pair.

D. Comparative study between static and mobile traps

The mobile trap algorithm with constant values of p_1 and p_2 is used for this study. The p_1 and p_2 values higher than those obtained for E117Q CA variant are used to generate the reaction data quickly. Two systems of number of particles along with two cases of relative mobility are studied. The particle systems are (1) excess number of mobile and stationary CA molecules over the number of zinc ions and (2) excess number of zinc ions over the number of stationary and mobile CA molecules. The relative mobility cases are (1) the zinc ions 24 times faster than the CA molecules, (2) the zinc ions 10 times faster than the CA molecules, and (3) the zinc ions 2 times faster than the CA molecules. First, the forward reaction is simulated and the k_{on} values are obtained. Then, the reversible reaction is simulated and the k_{off} values are obtained. After this first round of simulations, the second stage of simulations is carried out to study the behavior of the reaction data from the static and the mobile trap methodologies. The relative mobility of zinc ions is kept constant at 2 and one of the reaction probability values is varied while keeping the other constant. These simulations are run to study the time at which the reaction data from the mobile traps deviate from the reaction data from the static traps.

III. RESULTS AND DISCUSSION

A. Verification of implementation

Mobile trap simulations were carried out for a generic reaction [Eq. (14)] with (6, 60, 20, and 30) and (12, 60, 200, and 60) as the initial numbers of A and B particles, respectively. The simulation domain was a $1\times1\times1$ μm^3, with

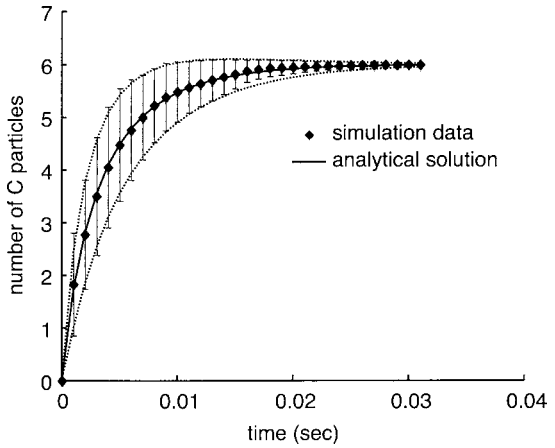

FIG. 2. Reaction data obtained from the mobile trap algorithm with a p_1 of 0.9. The numbers and diffusion coefficients of particles of types A and B are 6 and 12 and 10^{-9} and 10^{-11} m^2/s, respectively. Reaction data were fitted with an analytical solution with k of 1.82×10^{10} M^{-1} s^{-1} and uncertainty of 54%.

periodic boundary conditions. Assumed diffusion coefficients were 10^{-9} and 10^{-11} m^2/s for species A and B, respectively. Particles of species B were assumed to be spheres of 20 Å radius; particles of species A were assumed to be negligibly small. Value δ was assumed to be 5% of the radius of the B particle. Simulations were carried for four different p_1 values: 0.9, 0.5, 0.1, and 0.001. Figure 2 shows a typical mobile trap data along with the analytical solution [Eq. (15)] and the uncertainty in k that would envelope the standard deviation bars [Eq. (17)], for p_1 value of 0.9. Figure 2 shows that the reaction data obtained from the mobile trap simulations satisfy the law of mass action and also give the uncertainty value in k (the on rate) that would be impossible to obtain using the diffusion approach.

B. Correlation between k_{on} and p_1

Properties of the E117Q variant of CA were used for this study.[25] The survival time of a zinc ion among a number of CA molecules was obtained using the mobile trap algorithm in a $1\times1\times1$ μm^3 domain with periodic boundary conditions. CA molecule concentrations of 0.1, 0.2, 0.3, 0.4, and 0.5 μM were simulated. Diffusion coefficients for CA molecules and zinc ions were assumed to be 9.18×10^{-11} and 2.20×10^{-9} m^2/s, respectively. The δ value for these simulations was taken as 1% of radius of the CA molecule. CA molecules were randomly distributed at $t=0$, and zinc ions were initialized at random points among CA molecules. For each initial configuration of CA molecules, five simulations were carried with five different initial positions of a zinc ion; 20 realizations were simulated, for each of three values of p_1, 0.05, 0.01, and 0.005. When the total number of simulations for a CA concentration value exceeded 100, all running simulations were halted, and results were tabulated. For CA concentrations of 0.1, 0.2, and 0.3 μM, 100 sequential simulations were performed. Due to the need to run parallel simulations on multiple processors for the 0.4 and 0.5 μM CA concentrations because of their computational intensity and high run times, the number of completed simulations was variable, depending on when completion of 100 simulations was reached. Thus, for the higher concentrations, the total number of simulations ranged from 100 to 133. Survival times for various CA concentrations are shown in Fig. 3; reaction rates (1/average survival time) versus CA concentrations are shown in Fig. 4. The k_{on} values corresponding to three p_1 values are listed in Table III. Figure 3 shows that the *survival time* versus [CA] data follows a rectangular hyperbolic trend and Fig. 4 shows that the *average reaction rate* versus [CA] data follows a linear trend as described by Eq. (19). A rectangular hyperbola is a much higher order curve than a straight line. By plotting the data in two such forms, it

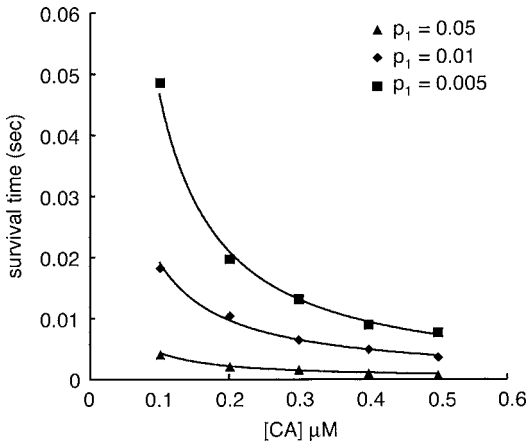

FIG. 3. Survival time vs concentration of CA with a rectangular hyperbola curve fit [per Eq. (19)] for three different p_1 values, 0.05, 0.01, and 0.005. Simulation times shown are average values for 100 realizations of each case.

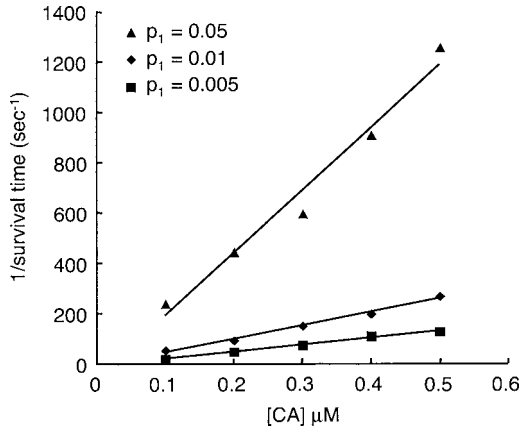

FIG. 4. Average reaction rate (1/survival time) vs concentration of CA with a straight-line curve fit [per Eq. (19)] for three different p_1 values, 0.05, 0.01, and 0.005. Simulation times shown are average values for 100 realizations of each case.

TABLE III. k_{on} values of CA-Zn reaction obtained using the straight lines as well the rectangular hyperbola method. Asterisks indicate unreported values.

p_1	k_{on} (M^{-1} s^{-1}) (straight line)	k_{on} (M^{-1} s^{-1}) (hyperbola)	Average k_{on} (M^{-1} s^{-1})	Experimental k_{on} (M^{-1} s^{-1})
0.05	2.49×10^9	2.37×10^9	2.43×10^9	*
0.01	5.35×10^8	5.27×10^8	5.31×10^8	*
0.005	2.78×10^8	2.55×10^8	2.66×10^8	2.95×10^8[a]

[a]Reference 25.

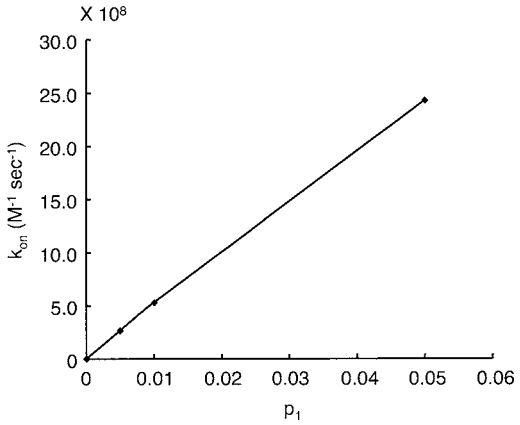

FIG. 5. A straight line passing through k_{on} vs p_1 data allows interpolation for a particular k_{on} value corresponding to a particular p_1 value.

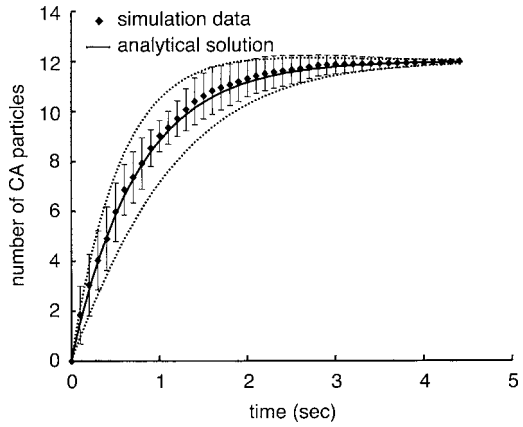

FIG. 6. A typical plot of the number of free CA molecules as a function of time, obtained from selective CA dissociation simulations, with 12 complex CA molecules, and p_1 and p_2 of 0.0055 and 6.5×10^{-6}, respectively. The time duration between two successive CA selections for dissociation was 4.25×10^{-7} s; the total simulated duration was 5 s. For this case, the k_{off} value is 1.342 s^{-1}, which is very close to the experimental k_{off} value of 1.3 s^{-1}.

can be seen that the on rate constants are very close (Table III), and thus the average of those values can be used to obtain the final correlation between the on rate and the reaction probabilities. Figure 5 shows that k_{on} versus p_1 data follow a linear relationship and hence the p_1 value corresponding to the k_{on} value of 2.95×10^{-8} M^{-1} s^{-1} can be obtained using interpolation and it is 0.0055.

C. Correlation between k_{off} and p_2

Again, the E117Q variant of CA was modeled, with a previously published value of k_{off} of 1.3 s^{-1}.[25] t_{dis} was obtained by running the mobile trap simulations for 1 s with p_1 of 0.005 and p_2 of 6×10^{-6} in a $1\times1\times1$ μm^3 volume domain and identical diffusion coefficients as for the p_1-k_{on} relationship. Twenty CA dissociation simulations were performed to obtain the number of free CA molecules as a function of time. k_{off} was obtained using these data and Eq. (20). The numbers of CA and zinc particles used for these simulations and corresponding t_{dis} and k_{off} values are shown in Table IV. The value of p_2 used in the mobile trap simulation was arrived at by trial and error, such that the t_{dis} value yielded the required k_{off} value. A typical plot of the number of the free CA molecules as a function of time is shown in Fig. 6. The k_{off} values in Table IV show that the moderate change in number particles has little effect on k_{off} values as long as p_1 and p_2 values are same.

D. Comparison with Gillespie's algorithm

Our mobile trap algorithm with 12 CA and 12 zinc particles was run for 1 s, with a p_1 of 0.0055 and p_2 of 6.5×10^{-6}. The number of particles (12) was calculated for a 20 nM concentration in a $1\times1\times1$ μm^3 domain, per published estimates of concentration of CA in live cells. The diffusion coefficients of CA molecules and zinc ions were as previously used in the $k_{on}-p_1$ study.

Gillespie's algorithm was run with 12 CA molecules and 12 zinc ions. k_{on} and k_{off} values for these simulations were 2.95×10^{8} M^{-1} s^{-2} and 1.3 s^{-1}, respectively; ten runs of each type of simulation were performed. Reaction data obtained from these simulations are shown in Fig. 7, with numbers of association and dissociation events contained in Table V. Table V and Fig. 7 show that the mobile trap algorithm delivers results similar to those obtained using our implementation of Gillespie's algorithm. This study further corroborates that the individual particle level probabilities, p_1 and p_2, are capable of modeling a chemical reaction.

E. Static versus the mobile traps

Two systems of particles were studied, with 20 zinc ions and 200 CA molecules, and 200 zinc ions and 20 CA molecules. Three cases of particle speed were selected, one with a D_{Zn} value of 2.19×10^{-9} m^2/s and a D_{CA} value of 9.18×10^{-11} m^2/s (i.e., with zinc ions 24 times faster than CA molecules, or the "fast zinc" case), the second with a D_{Zn} value of 9.18×10^{-10} m^2/s and a D_{CA} value of 9.18×10^{-11} m^2/s (i.e., with zinc ions 10 times faster than CA molecules, or the "slow zinc" case), and the third with a D_{Zn} value of 1.83×10^{-10} m^2/s and a D_{CA} value of

TABLE IV. k_{off} values for various initial numbers of CA and zinc particles. These data were obtained from the mobile trap implementation and the selective CA dissociation simulations.

No. of zinc ions	No. of CA molecules	t_{dis} (s)	p_1/p_2	k_{off} (s^{-1})	Uncertainty in k_{off} (%)
10	20	4.12×10^{-7}	$0.005/6\times10^{-6}$	1.46	45
12	12	4.25×10^{-7}	$0.0055/6.5\times10^{-6}$	1.34	40
20	30	2.17×10^{-7}	$0.005/6\times10^{-6}$	1.46	33
30	60	1.34×10^{-7}	$0.005/6\times10^{-6}$	1.52	35

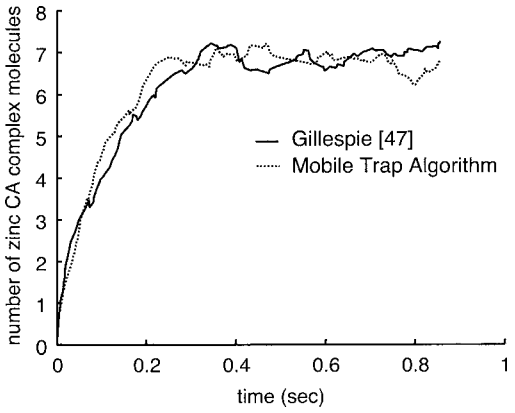

FIG. 7. Comparison between reaction data obtained from our implementation of Gillespie's algorithm and the mobile trap simulations. The numbers of CA and zinc particles were 12 each, and the simulated duration was 1 s. Data represent average values for ten realizations for each case.

9.18×10^{-11} m^2/s (i.e., with zinc ions 2 times faster than CA molecules, or the slow zinc case). The values of probabilities, p_1 and p_2, were 0.055 and 6.5×10^{-4}, respectively. Thus, higher values of p_1 and p_2 than those obtained for E117Q variant allowed efficient generation of comparative reaction data.

For stationary CA simulations, the diffusion coefficient of the CA molecule was added to the diffusion coefficient of a zinc ion. First, the forward reaction was simulated to study the effect of particle number-zinc speed configuration k_{on} values. Then the reversible reaction was simulated using the (p_1,p_2) pair.

Figures 8(a) and 8(b) show the numbers of complex zinc-CA molecules as a function of time for fast and slow zinc ions, respectively, reacting with excess stationary and mobile CA molecules in the forward CA-Zn reaction. Table VI shows k_{on} and the numbers of particles associated with these reactions for each case. Figures 9(a) and 9(b) show the number of complex zinc-CA molecules as a function of time for fast and slow zinc ions, respectively, reacting with excess mobile and stationary CA molecules in the reversible CA-Zn reaction. The corresponding values of k_{off} are shown in Table VII.

Figures 8 and 9 reveal the importance of exploring the effect of static trap and mobile trap approaches when the zinc ions have different mobilities. Biometal ions such as zinc are detected using the protein-based sensors such as CA. To detect the sources and sinks of zinc ions in a cellular medium, the mobile sensor CA molecules are used and these molecules fluoresce (with the help of a fluorescent ligand) when they bind to the mobile zinc ions. In a cell a large number of other zinc-binding proteins and ligands exist; therefore obtaining reaction probabilities is a better way to understand how a typical protein molecule acquires a zinc ion, a rare species.

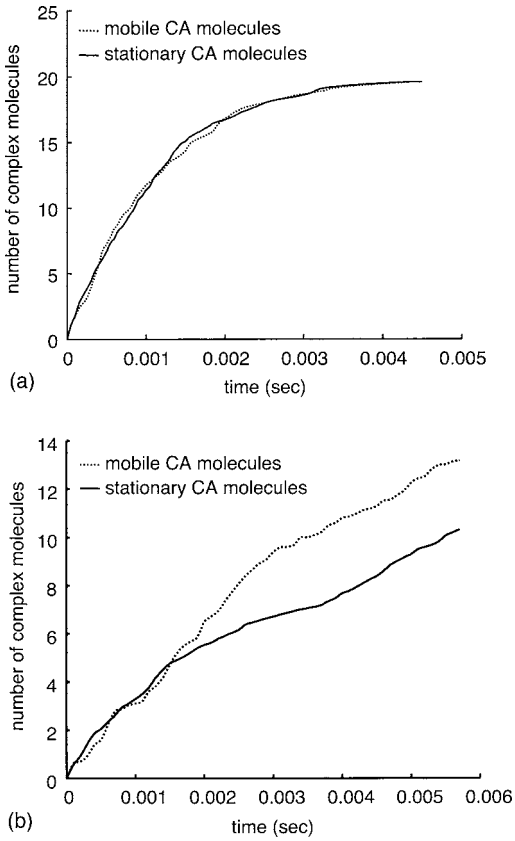

FIG. 8. Number of complex CA-Zn molecules as a function of time when 20 zinc molecules react with a hypothetical variant of CA having a p_1 of 0.055 via the forward CA-Zn reaction. The number of CA molecules is 200. Reaction curves are shown for stationary (solid) and mobile (dotted) CA molecules. Cases shown are for fast zinc ions reacting with CA molecules (a) and slow zinc ions reacting with CA molecules (b).

Figure 8(a) shows reaction data curves obtained using the static trap and the mobile trap approaches. The small difference (<10%) [Table VI(a)] in the k_{on} values for all four cases of fast zinc-CA reaction shows that the static and

TABLE V. Average numbers of CA-Zn association events and complex CA dissociation events from ten mobile trap and Gillespie-type simulations. For the mobile trap simulations, p_1 and p_2 values were 0.0055 and 6.5×10^{-6}, respectively. For Gillespie's algorithm simulations, k_{on} and k_{off} values were 2.95×10^8 $M^{-1}s^{-1}$ and 1.3 s^{-1}, respectively.

Algorithm	Average number of associations (standard deviation)	Parameter Average number of dissociations (standard deviation)	p_1	p_2
Mobile trap algorithm	15.6 (2.5)	7.9 (2.4)	0.0055	6.5×10^{-6}
Gillespie implementation[a]	15.8 (2.3)	9.0 (1.8)	Variable	Variable

[a]Reference 47.

TABLE VI. The on rate constant values for CA-Zn reactions involving (a) fast zinc ions reacting with mobile and stationary CA molecules and (b) slow zinc ions reacting with mobile and stationary CA molecules. The probability of association is 0.055 in each case.

	No. of CA molecules	No. of zinc ions	D_{CA} (m^2/s)	D_{Zn} (m^2/s)	k_{on} ($M^{-1}\,s^{-1}$)
(a)	20	200	0	2.29×10^{-9}	2.66×10^{9}
	20	200	9.18×10^{-11}	2.19×10^{-9}	2.67×10^{9}
	200	20	0	2.29×10^{-9}	2.90×10^{9}
	200	20	9.18×10^{-11}	2.19×10^{-9}	2.83×10^{9}
(b)	20	200	0	2.75×10^{-10}	2.88×10^{8}
	20	200	9.18×10^{-11}	1.83×10^{-10}	3.32×10^{8}
	200	20	0	2.75×10^{-10}	3.98×10^{8}
	200	20	9.18×10^{-11}	1.83×10^{-10}	5.16×10^{8}

the mobile trap algorithms give essentially the same results. On the other hand, Fig. 8(b) shows that the reaction data curves produce similar results only for the initial 1.8 ms, whereupon results diverge. The substantial difference ($>10\%$) in the k_{on} values (Table VI) for all four cases of slow zinc-CA reaction shows that the static trap approach yields relatively slower reaction rates, and thus will generally overestimate the reaction probability.

Figures 9(a) and 9(b) show that the saturation point obtained by the static trap algorithm is higher than the one obtained using the mobile trap algorithm. Also, the off rate values obtained using the static trap approach are lower than those obtained using the mobile trap approach (Table VII).

The data in Figs. 8(b), 9(a), and 9(b) were also analyzed using curve fitting to check the long time behavior exponent. These data follow the general equation

$$\mathrm{CA}(t) = A(1 - e^{-Bt}), \tag{22}$$

where A and B are constants. Hence instead of plotting the data in log-log scale, Eq. (22) was curve fitted and the values of constants A and B are shown in Table VIII. It can be seen that the data in these figures are characterized not only by different exponents (B values) but also by the A values. And the A values represent the saturation point of the reactions.

This study also revealed that the reaction data curve using the static and the mobile trap approaches deviate after some time (we call this point of time as *deviation time* or *time of deviation*). This point of time was studied by simulating Zn-CA association and dissociation reactions with static and mobile CA molecules. The relative zinc mobility was 2 and the values of the reaction probabilities for different simulations are shown in Table IX (italic and nonbold values). The deviation time values were also recorded from the simulations that were ran for different relative zinc mobilities. All simulation parameters and the corresponding deviation times are shown in Table IX.

Figure 10(a) shows the normalized time of deviation plotted as a function of relative zinc mobility. The normalized time of deviation was obtained as follows:

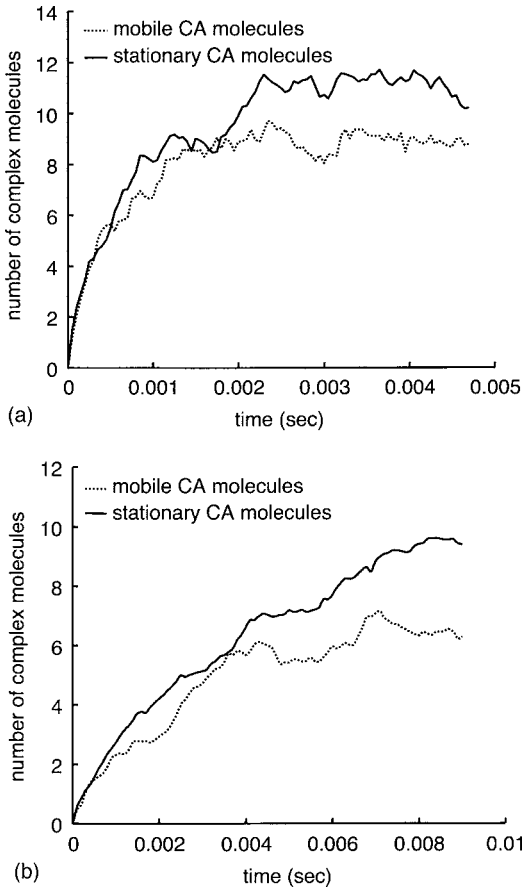

FIG. 9. Number of complex CA-Zn molecules as a function of time when 200 zinc ions react with 20 CA molecules in the reversible reaction. The reaction curves are for stationary CA (solid curve) as well as mobile CA (dotted curve) molecules. The p_1 value was 0.055 and the p_2 value was 6.5×10^{-4}. Cases shown are for fast zinc ions reacting with CA molecules (a) and slow zinc ions reacting with CA molecules (b).

$$T_d = \frac{t_d D_{Zn}}{L^2}, \tag{23}$$

where T_d is the normalized time of deviation, t_d is the deviation time obtained from the simulations, D_{Zn} is the diffusion coefficient of zinc ions, and L is the length of the simulation domain. T_d versus relative zinc mobility data follow a straight line. Thus as zinc ion diffusivity becomes comparable to the protein molecules, the static trap and the mobile trap approaches deviate quickly and one must resort to the mobile trap approach for correct interpretation of the experimental results.

Figure 10(b) shows the reciprocal of the deviation time plotted as a function of the probability of association. These data also follow a straight line; conversely the product of the deviation time and the association probability is a constant. This finding suggests that for a slowly reacting protein sensor, the static and the mobile trap methodology matters for proper interpretation while for a very reactive protein sensor, it does not. In practice, it is very difficult to make a protein sensor with a p_1 value of close to 1 (which would lead to diffusion controlled reaction rate) and this study reveals the importance of the mobile trap methodology. Figure 10(c) shows the deviation time plotted as a function of the prob-

TABLE VII. On rate and off rate constants for CA-Zn reactions involving fast and slow zinc ions reacting with mobile and stationary CA molecules.

No. of CA molecules	No. of zinc ions	D_{Zn} (m^2/s)	D_{CA} (m^2/s)	k_{on} ($M^{-1}\ s^{-1}$)	k_{off} (s^{-1})
20	200	2.29×10^{-9}	0.0	2.66×10^{9}	1031
20	200	2.19×10^{-9}	9.18×10^{-11}	2.67×10^{9}	1584
20	200	2.75×10^{-10}	0.0	2.88×10^{8}	117.1
20	200	1.83×10^{-10}	9.18×10^{-11}	3.37×10^{8}	268.7

ability of dissociation. These data do not show the straight line trend and the deviation time is small for the two extreme p_2 values.

The results of static versus mobile trap methodology can be summarized as follows. Protein-based sensors, such as CA molecules, are either expressed or injected into a cell. These sensors diffuse into the cell and bind ions whenever they encounter the ions they are sensing. When such ion-bound sensors are excited, they emit fluorescence. The fluorescence yield is read against a precalibrated scale to quantify the number of ions and hence the ionic concentration. Ideally, the number of sensors should be much larger than the expected maximum number of free/exchangeable ions. But there is a cost associated with injecting/expressing a protein sensor and a live cell will limit the number of sensors it can admit. If the sensor molecules have very low dissociation constant and very high association constant, then the number of ions bound to the sensors is not a true measure of available number ions. For a tightly regulated species, such as zinc ions, the cell will actuate its homeostasis mechanism to make the necessary number of ions available for the cellular activities. Hence the sensors are required to associate and dissociate with the ions relatively quickly and the fluorescence from such a sensor-ion reaction at equilibrium can be used as a measure of the number of ions. From the basics of probability, it is clear that a fraction of the total zinc population will be sensed. To estimate the number of zinc ions present in the system so as to obtain the number of bound ones, one can either simulate the sensor-ion reaction using the static trap or the mobile trap methodology. The static trap methodology has been employed classically[49] but experimental data necessarily result from traps that are physically mobile (CA molecules). Thus for a given fluorescence and with association-dissociation reactions between ions and sensors, the static trap approach systematically underestimates the number of zinc ions present in the system.

TABLE VIII. The values of constants obtained from curve fitting Eq. (22) in Figs. 8(b), 9(a), and 9(b) data. These values show that the reaction data from the static trap and the mobile trap methodologies are characterized by different exponents and the saturation points.

Figure	Static trap (A/B)	Mobile trap (A/B)
8(b)	12.18/282.6	19.27/204.1
9(a)	11.09/1371	8.69/1899
9(b)	10.88/228.7	6.89/368.1

F. Contrast with the well-stirred hypotheses and general implications of work

Though we can conceive of a mathematical framework for well-stirred systems, i.e., systems in which all species are distributed as Poisson points, such a framework is only a base line at best, for real systems. Green's function solutions for closed-form probabilities of association of heterogeneous mixtures might be available; yet the boundary conditions for locations and rates of sources and sinks in the cell will ultimately require detailed simulation based on nanoscale imaging. Thus, rather than pursue a closed-form solution for such a system, we instead focused on the stochastic problem because of its flexibility in application to realistic situations. The present mobile trap algorithm is developed as an integrated approach that simulates a reaction between particles using their spatial positions and the temporal probability of being in a particular state into account. Our findings demonstrated this approach to be both fast and capable of reproducing other less-refined techniques. Perhaps most importantly, our results demonstrate that experimental data can be seamlessly incorporated into this framework.

G. Implications of findings for intracellular modeling of zinc transport and comparisons with other approaches

When reactant concentrations are very small, particle flux in describing motion cannot be used. All such particles interact with each other that eventually give rise to the chemical reaction involving the reactants and products. At the particle level, the concept of concentration is replaced by the probability of existence of the particle at a distance x at time t, $p(x,t)$. Theoretically, an equation of motion such as Eq. (24) could be written for each particle and possible association/dissociation events could be monitored.

$$\frac{\partial p(x,t)}{\partial t} = D\frac{\partial^2 p(x,t)}{\partial x^2}. \tag{24}$$

Thus one must use probabilistic techniques to rationally model chemical reactions at very small reactant concentrations.

Indeed, solution of linear equations to produce diffusion coefficients belies a great deal of complexity in the atomistic and molecular interactions that determine the fate of ions. Building upon very early and clever work by von Smoluchowski,[49] generations of workers have employed "rule-based" models for interactions of species in modeling chemical kinetics. This theory has been used to model ionic

TABLE IX. The values of parameters used to simulate Zn-CA association-dissociation reactions using the static trap and the mobile trap approaches. The values of the deviation times were obtained using simulations.

No. of CA molecules	No. of zinc ions	D_{Zn} (m^2/s)	D_{CA} (m^2/s)	p_1	p_2	Deviation time (s)
20	**200**	$\mathbf{2.19\times10^{-9}}$	$\mathbf{9.18\times10^{-11}}$	**0.055**	$\mathbf{6.5\times10^{-4}}$	**0.0018**
20	**200**	$\mathbf{1.83\times10^{-10}}$	$\mathbf{9.18\times10^{-11}}$	**0.055**	$\mathbf{6.5\times10^{-4}}$	**0.0021**
20	**200**	$\mathbf{9.18\times10^{-10}}$	$\mathbf{9.18\times10^{-11}}$	**0.055**	$\mathbf{6.5\times10^{-4}}$	**0.0036**
20	*200*	1.83×10^{-10}	9.18×10^{-11}	*0.55*	6.5×10^{-4}	*No separation*
20	*200*	1.83×10^{-10}	9.18×10^{-11}	*0.0055*	6.5×10^{-4}	*0.003*
20	200	1.83×10^{-10}	9.18×10^{-11}	0.055	6.5×10^{-3}	0.0012
20	200	1.83×10^{-10}	9.18×10^{-11}	0.055	6.5×10^{-5}	0

as well as colloidal systems[30,50] and can account for long-range interparticle potentials.[33] This theory has been the basis for the protein-protein simulation method.[34] von Smoluchowski theory gives the maximum possible k_{on} value (also referred to as the diffusion controlled rate constant), and modifications such as the probability of association upon collision[34] and uses of an effective radius (smaller than the physical radius)[51] have been suggested to account for experimentally observed rates[49] (e.g., for the CA-zinc system, the diffusion controlled rate constant is about 4.418×10^{10} M^{-1} s^{-1} but the experimentally observed maximum on rate constant is 2.95×10^{8} M^{-1} s^{-1}). The concentration-based diffusion approach (von Smoluchowski theory) models association rate between reactant particles using the flux of one reactant molecule, say, A, at a surface, called the reaction surface of radius R of the second reactant molecule, say, B, that is stationary and at the origin of the system. This approach does not track the individual particle movement and also it does not account for possible dissociation of product molecules.

When the number of reactant particles is very low, concentration must be replaced by the probability distribution of particle positions. This method used the basic diffusion equations and the concentration was replaced by the probability distribution to obtain the time dependent evolution of probability of finding a particle at a particular location.[59] For 2D or 3D reaction space, either targets were stationary or traps were stationary. The relative motion was accounted using the effective coefficient of diffusion.[42] The limitation of this method is that in the real world, a physical reaction takes place with mobile traps and mobile targets and their motion is random and uncorrelated. The particle motion does take place in the continuum and in three-dimensional space and under these conditions, it is difficult to solve the probability equations that are set up using this method.

Brownian dynamics simulations estimated the probability of association between a pair of an enzyme molecule (protein) and a substrate (an ion).[33,34] This probability was used to estimate the *on rate constant* using the diffusion-controlled rate. The motion of individual particles was modeled as Brownian motion with friction effects. This method considered the directed nature of substrate binding site on the enzyme molecule. The enzyme molecule was stationary during the simulation and only one pair was simulated. This method did not model random motion of the enzyme molecule. Because of very small time increments, it is computationally intensive to simulate a reaction between mobile reactant particles.

Gillespie's algorithm[47] has been extensively used to study the fluctuations in the reaction data. This method is very useful when reactant to product path consists of a large number of intermediate reactions and the variation in the

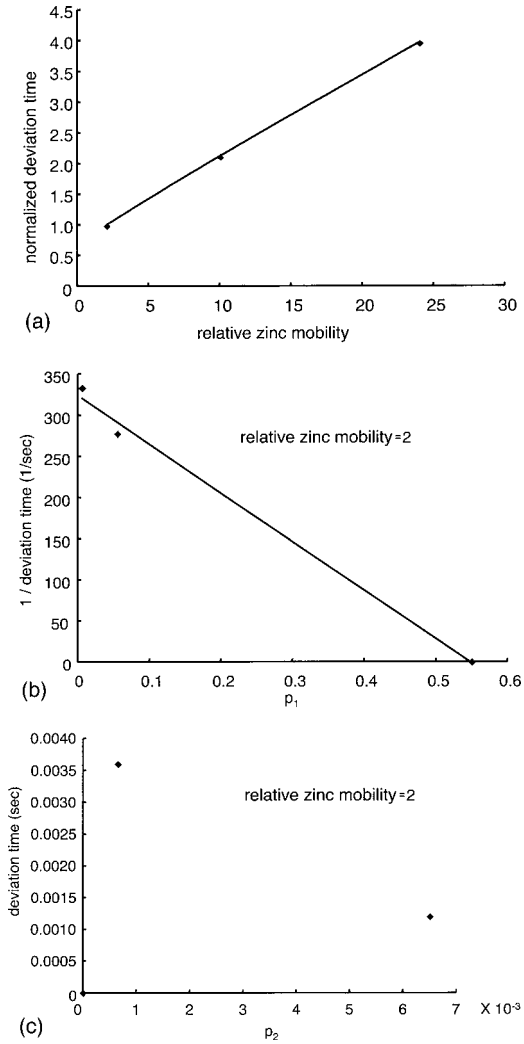

FIG. 10. The point of time (deviation time) at which the reaction data from the mobile trap and the static trap methodology deviate from each other, plotted as a function of relative zinc mobility, the probability of association and dissociation; (a) normalized time of deviation as a function of relative zinc mobility, (b) reciprocal of deviation time as a function of the probability of association, and (c) deviation time as a function of the probability of dissociation.

product concentrations affects the system behavior. This method does not consider the fate of an individual molecule nor does it consider the spatial positions of reactant particles. Another alternative method that can simulate the fluctuations in the reaction data is the STOCHSIM algorithm.[48] This method tracks the fate of individual reactant particles. The recent version can model simple 2D structures and interaction between two nearest neighbor particles. This algorithm is equivalent to Gillespie's algorithm. Both Gillespie's algorithm and STOCHSIM use k_{on}, k_{off} values as well as the current number of reactant and product molecules to calculate the probability of forward and backward reactions. These probabilities are not defined for individual particles but rather are the global probabilities. Hence strictly speaking, these algorithms do not model probabilistic association and dissociation on an individual particle basis.

Monte Carlo methods are nothing but the numerical solutions to simulate probability-based diffusion approach at particle level. The method of static traps has been used to determine the survival time of a target in 3D.[38,39] This survival time was a measure of the rate constant of trap-target reaction. In its probabilistic binding variation,[40] this method has been used to simulate trapping of a target by static traps with a probability of association of other than 1. This method tracks the motion of individual particles and their fate but still, the traps are immobile.

The Monte Carlo mobile trap-mobile target approach has been implemented in continuum[36] as well as on the grid.[35,54] A continuum study was carried out to simulate irreversible diffusion controlled reactions in two dimensions with particles executing Pearsonian random walk. The grid study was carried out to understand the kinetics (Michaelis-Menten) in a fractal medium, simulating association and dissociation reactions. As a variation, this method has been used to simulate binding of receptors to a substrate in the form of a flat surface.[70] The limitations of these approaches have been addressed earlier.

The presumed low concentration of intracellular zinc stems from the relatively recent experimental work, in which the concentration of free intracellular zinc was estimated by observing the response of the zinc uptake pump protein ZnuC and the zinc excursion pump protein ZntR regulators in *E. coli*.[3] In these experiments, it was observed that the increase in free zinc concentration suppressed ZnuC expression and increased ZntR expression. The switchover point at which those activities took place was found to be at $10^{-15}M$ free zinc concentration. When compared to the concentration of one zinc ion in *E. coli*. 1 nM, the switchover point was very small, and hence it was concluded that there was virtually no free zinc in *E. coli*. But if we assume a spherical *E. coli* bacterium, and further assume free diffusion of a protein molecule such as CA, the expected time that a protein would take to reach the surface starting from the origin would be of the order of millisecond. These travel times can be estimated using the studies that showed that the apparent diffusion coefficient of a protein through the cell was of the order of 10^{-12} m^2/s.[71,72] Study of diffusion of protons also revealed a diffusion coefficient of $\sim 10^{-11}$ m^2/s.[73] As a limiting case, if we assume that the diffusion coefficient of zinc ions is the same as that of protons, then in *E. coli*, the time required for a protein to travel a distance of 0.62 mm (radius of *E. coli* based on 10^{-15} l volume of the sphere) is of the order of 0.192 s and for a zinc ion it is of the order of 0.0192 s.

This prior work assumed, but did not establish, that the regulatory proteins ZnuC and ZntR were "fast" enough to sense extra free zinc ions in the cellular environment thus leading to an underestimate of the "free zinc" concentration. Recently the intracellular free zinc concentration in eukaryotic cells was estimated at 10 pM using the CA-based sensors under conditions where zinc binding was at a steady state. In general, the term free zinc might properly be recast as "readily exchangeable zinc," in the mathematical sense, since, as recently discussed by Sastry and Lastoskie,[62] the putatively low concentrations of intracellular zinc ions are tightly regulated and are thus the subject of competition for a multitude of binding proteins within the cell. These issues, collectively, suggest use of stochastic modeling for zinc-protein interaction.

IV. CONCLUSIONS AND FUTURE WORK

A mobile trap algorithm was implemented for a general $(A+B)$ case and was verified, i.e., probability-based simulations were shown to satisfy the law of conservation of mass. A specific CA-zinc reaction was also simulated via the mobile trap approach. The probability pair (p_1,p_2) was postulated to be a forward mapping for the kinetic constants (k_{on},k_{off}) in each case.

Implementation of this mobile trap algorithm revealed that accounting for mobility in both sensors and ions is important, when their mobilities are similar (i.e., zinc ions and CA molecules). Specifically, we found that a ratio of the mobilities for ion/sensor equal to two resulted in deviations between static, and mobile trap simulations. For the specific case of ionic, intracellular zinc, which has relatively low mobility inside a cell due to chelating tendency of the proteins in the cell, the mobile trap approach appears more suitable. Also, the present understanding in prior work is that the number of free zinc ions in a cell is very small. Though zinc is the second most abundant biometal in humans, intracellular ionic zinc concentrations have been found to be vanishingly low. It seems clear that zinc is tightly bound, and probably competed for, by a number of proteins. The mobile trap algorithm is particularly well-suited to map the outcomes of this putative competition, because the particular mobilities of protein "competitors" can be accounted for, directly. There is the additional possibility that zinc is sequestered at specific locations in a cell, and that the environment is not spatially homogenous, either in traps or targets. Again, the mobile trap algorithm can be used to directly simulate such inhomogenous domains.

The association methology adopted in this algorithm also suggests a more general, theoretical means to estimate the collision frequency. The approach involves use of a likelihood of minimum distance between the particles and distribution of the minimum distance, after a specified time, to predict binding events.

These findings may have broader implications and util-

ity, for intracellular modeling. The approach of characterizing a protein molecule by the probabilities of association and dissociation makes no assumptions about is spatial position. Further, the presence of cytoskeleton, endoplasmic reticulum, and other organelles, along with viscosity gradients and anisotropy of the cell interior, can be directly modeled, with improvements in computational processing speeds. This methodology, in conjunction with advancements in sensing technology,[74] cluster statistics for sensor-type particles,[75–77] and mapping of nano-fiber networks,[78,79] may be employed to estimate the probability of sensing a rare species with specific sensors, and enable improved sensor design.

We are presently modifying our existing algorithm, to simulate competitive binding between two types of protein molecules, and more specifically, per the points raised above, to simulate rate experiments on zinc and CA.[80] The ultimate aim is to allow the seamless integration of atomistic simulations with characterization of protein interactions, which is not possible with prior models. The pair association/dissociation probabilities (p_1,p_2) mathematically characterizes a protein molecule completely, and can be readily extended to simulate the competition of multiple proteins for very few targets, after characterization of probabilities from atomic simulations. Further, the probabilities p_1 and p_2 immediately map to experimental kinetic constants. Thus, we anticipate that this general approach will ultimately allow direct comparison of experimental and atomistic simulations in a single, statistically robust framework.

ACKNOWLEDGMENTS

Support for this work provided by the W. M. Keck Foundation to three of the authors (A.M.S., C.M.L. and C.A.F.) and the National Science Foundation through an NSF PECASE to the last author (A.M.S.) is gratefully acknowledged. Computations were performed on a Sun Fire Cluster V480, a gift of Sun Microsystems, Incorporated to two of the authors (C.M.L. and A.M.S.). The authors also gratefully acknowledge this equipment support.

APPENDIX: DERIVATION OF THE NUMBER OF COMPLEX CA MOLECULES AS A FUNCTION OF TIME USING TWO APPROACHES OF SELECTIVE CA DISSOCIATION

The approach of checking each CA molecule for dissociation and the presently implemented approach of randomly selecting a CA molecule for dissociation are equivalent. This can be proved using the basic probability theory. We start with a group of n complex (zinc bound) CA molecules and go on dissociating them one after another using these two methods.

Method 1: Checking all complex CA molecules for dissociation. Let the probability of dissociation of a complex CA molecule upon selection be p. After the first turn of checking, the expected number of CA molecules that will be dissociated is pn. Hence the number of complex CA molecules after the first turn of dissociation is

$$n_1 = n - pn = n(1-p). \tag{A1}$$

After the second turn of dissociation checking, the number of complex CA molecules can be estimated using the above procedure and it is

$$n_2 = n_1 - pn_1 = n(1-p) - p(1-p)n = n(1-p)^2. \tag{A2}$$

After the mth turn of dissociation checking, the number of complex molecules is

$$n_m = n(1-p)^m \approx ne^{-pm}. \tag{A3}$$

Method 2: Selecting a CA molecule at random and checking it for dissociation. It is easy to derive an expression for n_m assuming that the ith turn of dissociation has taken place. Let the number of complex CA molecules be n_i and the number of free CA molecules be n_{fi}. The initial number of CA molecules is n. Let the probability of dissociation of a complex CA molecule be p_2 (to distinguish it from p used in Method 1). The number of complex CA molecules after the $i+1$th turn is

$$n_{i+1} = n_i\frac{n-n_i}{n} + n_i\frac{n_i}{n}(1-p_2) + (n_i-1)\frac{n_i}{n}p_2, \tag{A4}$$

$$n_{i+1} = n_i\left(1-\frac{p_2}{n}\right). \tag{A5}$$

We can obtain the expressions for $n_1,n_2,\ldots,n_m$ using Eq. (A5) and they are as follows:

$$n_1 = n\left(1-\frac{p_2}{n}\right), \tag{A6}$$

$$n_2 = n_1\left(1-\frac{p_2}{n}\right) = n\left(1-\frac{p_2}{n}\right)^2, \tag{A7}$$

$$n_m = n\left(1-\frac{p_2}{n}\right)^m = ne^{-p_2 m/n}. \tag{A8}$$

From Eqs. (A3) and (A8), it can be seen that

$$p = p_2/n. \tag{A9}$$

Selecting a random CA molecule for dissociation is more efficient because it saves the physical time required for a simulation run.

[1] D. Beyersmann and H. Haase, BioMetals **14**, 331 (2001).
[2] K. Yamamoto and A. Ishihama, J. Bacteriol. **187**, 6333 (2005).
[3] C. E. Outten and T. V. O'Halloran, Science **292**, 2488 (2001).
[4] T. J. B. Simons, J. Membr. Biol. **123**, 63 (1991).
[5] D. Atar, P. H. Backx, M. M. Appel, W. D. Gao, and E. Marban, J. Biol. Chem. **270**, 2473 (1995).
[6] J. Benters, U. Flögel, T. Schäfer, D. Leibfritz, S. Hechtenberg, and D. Beyersmann, Biochem. J. **322**, 793 (1997).
[7] S. L. Sensi, L. M. T. Canzoniero, S. P. Yu, H. S. Ying, J. Y. Koh, G. A. Kerchner, and D. W. Choi, J. Neurosci. **17**, 9554 (1997).
[8] H. Haase and D. Beyersmann, BioMetals **12**, 247 (1999).
[9] R. A. Bozym, R. B. Thompson, A. K. Stoddard, and C. A. Fierke, ACS Chem. Biol. **1**, 103 (2006).
[10] B. L. Vallee and K. H. Falchuk, Physiol. Rev. **73**, 79 (1993).
[11] E. H. Cox and G. L. McLendon, Curr. Opin. Chem. Biol. **4**, 162 (2000).
[12] D. S. Auld, BioMetals **14**, 271 (2001).
[13] H. Lodish, A. Berk, S. L. Zipursky, P. Matsudaira, D. Baltimore, and J. Darnell, *Molecular Cell Biology*, 4th ed. (Freeman, New York, 2000).

[14] T. Lynch, R. A. Cherny, and A. I. Bush, Exp. Gerontol. **35**, 445 (2000).
[15] J. H. Weiss, S. L. Sensi, and J. Y. Koh, Trends Pharmacol. Sci. **21**, 395 (2000).
[16] C. J. Frederickson and A. I. Bush, BioMetals **14**, 353 (2001).
[17] R. E. Safford and J. B. Bassingthwaighte, Biophys. J. **20**, 113 (1977).
[18] B. M. Slepchenko and F. Bronner, Am. J. Physiol.: Cell Physiol. **281**, C270 (2001).
[19] K. Nakatani, C. Chen, and Y. Koutalos, Biophys. J. **82**, 728 (2002).
[20] C. A. Fierke and R. B. Thompson, BioMetals **14**, 205 (2001).
[21] R. A. Bozym, R. B. Thompson, and C. A. Fierke, Biophys. J. **86**, 606A (2004).
[22] L. L. Kiefer and C. A. Fierke, Biochemistry **33**, 15233 (1994).
[23] L. L. Kiefer, S. A. Paterno, and C. A. Fierke, J. Am. Chem. Soc. **117**, 6831 (1995).
[24] J. A. Ippolito, T. T. Baird, S. A. McGee, D. W. Christianson, and C. A. Fierke, Proc. Natl. Acad. Sci. U.S.A. **92**, 5017 (1995).
[25] C. C. Huang, C. A. Lesburg, L. L. Kiefer, C. A. Fierke, and D. W. Christianson, Biochemistry **35**, 3439 (1996).
[26] C. A. Lesburg, C. C. Huang, D. W. Christianson, and C. A. Fierke, Biochemistry **36**, 15780 (1997).
[27] J. A. Hunt and C. A. Fierke, J. Biol. Chem. **272**, 20364 (1997).
[28] R. B. Thompson, M. L. Cramer, R. Bozym, and C. A. Fierke, J. Biomed. Opt. **7**, 555 (2002).
[29] K. A. McCall and C. A. Fierke, Biochemistry **43**, 3979 (2004).
[30] P. Bongrand, Rep. Prog. Phys. **62**, 921 (1999).
[31] H. Gutfreund, *Kinetics for the Life Sciences: Receptors, Transmitters and Catalysts* (Cambridge University Press, Cambridge, 1995).
[32] A. Fersht, *Enzyme Structure and Mechanism* (Freeman, New York, 1985).
[33] S. H. Northrup, S. A. Allison, and J. A. McCammon, J. Chem. Phys. **80**, 1517 (1984).
[34] S. H. Northrup and H. P. Erickson, Proc. Natl. Acad. Sci. U.S.A. **89**, 3338 (1992).
[35] H. Berry, Biophys. J. **83**, 1891 (2002).
[36] J. Martins, K. R. Naqvi, and E. Melo, J. Phys. Chem. B **104**, 4986 (2000).
[37] L. H. Zheng and Y. C. Chiew, J. Chem. Phys. **90**, 322 (1989).
[38] S. Torquato and I. C. Kim, Appl. Phys. Lett. **55**, 1847 (1989).
[39] S. B. Lee, I. C. Kim, C. A. Miller, and S. Torquato, Phys. Rev. B **39**, 11833 (1989).
[40] M. R. Riley, H. M. Buettner, F. J. Muzzio, and S. C. Reyes, Biophys. J. **68**, 1716 (1995).
[41] A. V. Popov and N. Agmon, J. Chem. Phys. **115**, 8921 (2001).
[42] M. Moreau, G. Oshanin, O. Bénichou, and M. Coppey, Phys. Rev. E **69**, 046101 (2004).
[43] A. D. Sánchez, M. A. Rodriguez, and H. S. Wio, Phys. Rev. E **57**, 6390 (1998).
[44] S. Redner and P. L. Krapivsky, Am. J. Phys. **67**, 1277 (1999).
[45] N. Agmon, J. Chem. Phys. **81**, 2811 (1984).
[46] P. M. Richards, J. Chem. Phys. **85**, 3520 (1986).
[47] D. T. Gillespie, J. Phys. Chem. **81**, 2340 (1977).
[48] C. J. Morton-Firth and D. Bray, J. Theor. Biol. **192**, 117 (1998).
[49] M. von Smoluchowski, as discussed in O. G. Berg and P. H. von Hippel Annu. Rev. Biophys. Biophys. Chem. **14**, 131 (1985).
[50] J. I. Steinfeld, J. S. Francisco, and W. L. Hase, *Chemical Kinetics and Dynamics* (Prentice-Hall, Englewood Cliffs, NJ, 1989).
[51] S. S. Andrews and D. Bray, Phys. Biol. **1**, 137 (2004).
[52] W. Shi, M. V. Inamdar, A. M. Sastry, and C. M. Lastoskie, J. Phys. Chem. C. (to be published).
[53] L. He and B. Niemeyer, Biotechnol. Prog. **19**, 544 (2003).
[54] T. E. Turner, S. Schnell, and K. Burrage, Comput. Biol. Chem. **28**, 165 (2004).
[55] A. Arkin, J. Ross, and H. H. McAdams, Genetics **149**, 1633 (1998).
[56] M. Yoshimi, Y. Osana, T. Fukushima, and H. Amano, *Field-Programmable Logic and Applications Proceedings* (Springer-Verlag, Berlin, 2004), Vol. 3203, pp. 105–114.
[57] A. Szabo, R. Zwanzig, and N. Agmon, Phys. Rev. Lett. **61**, 2496 (1988).
[58] H. Kim and K. J. Shin, Phys. Rev. Lett. **82**, 1578 (1999).
[59] H. C. Berg, *Random Walks in Biology*, expanded ed. (Princeton University Press, Princeton, NJ, 1993).
[60] S. Redner, *A Guide to First-Passage Processes* (Cambridge University Press, Cambridge, 2001).
[61] A. Rojnuckarin, D. R. Livesay, and S. Subramaniam, Biophys. J. **79**, 686 (2000).
[62] A. M. Sastry and C. M. Lastoskie, Philos. Trans. R. Soc. London, Ser. A **362**, 2851 (2004).
[63] Y. B. Yi, H. Wang, A. M. Sastry, and C. M. Lastoskie, Phys. Rev. E **72**, 021913 (2005).
[64] J. S. van Zon and P. R. ten Wolde, Phys. Rev. Lett. **94**, 128103 (2005).
[65] www.pdb.org
[66] H. Motulsky and A. Christopoulos, *Fitting Models to Biological Data Using Linear and Nonlinear Regression: A Practical Guide to Curve Fitting* (Oxford University Press, New York, 2004).
[67] J. R. Partington, *A Short History of Chemistry*, 2nd ed. (MacMillan, London, UK, 1957).
[68] J. P. Holman, *Experimental Methods for Engineers*, 6th ed. (McGraw-Hill, New York, 1994).
[69] I. V. Gopich and A. Szabo, J. Chem. Phys. **117**, 507 (2002).
[70] A. L. Edelstein and N. Agmon, J. Comput. Phys. **132**, 260 (1997).
[71] M. B. Elowitz, M. G. Surette, P. E. Wolf, J. B. Stock, and S. Leibler, J. Bacteriol. **181**, 197 (1999).
[72] B. N. Kholodenko, G. C. Brown, and J. B. Hoek, Biochem. J. **350**, 901 (2000).
[73] P. Swietach, M. Zaniboni, A. K. Stewart, A. Rorrini, K. W. Spitzer, and R. D. Vaughan-Jones, Prog. Biophys. Mol. Biol. **83**, 69 (2003).
[74] I. Rasnik, S. A. McKinney, and T. Ha, Nat. Methods **3**, 891 (2006).
[75] Y. B. Yi and A. M. Sastry, Phys. Rev. E **66**, 066130 (2002).
[76] Y. B. Yi and A. M. Sastry, Proc. R. Soc. London, Ser. A **460**, 2353 (2004).
[77] Y. B. Yi, C. W. Wang, and A. M. Sastry, J. Electrochem. Soc. **151**, A1292 (2004).
[78] A. M. Sastry, C. W. Wang, and L. Berhan, Key Eng. Mater. **200**, 229 (2001).
[79] Y. B. Yi, L. Berhan, and A. M. Sastry, J. Appl. Phys. **96**, 1 (2004).
[80] N. Westerberg and C. A. Fierke (unpublished).